VOL.98 NO.SM11. NOV. 1972

JOURNAL OF THE SOIL MECHANICS AND FOUNDATIONS DIVISION

PROCEEDINGS OF
THE AMERICAN SOCIETY
OF CIVIL ENGINEERS

VOL.98 NO.SM11. NOV. 1972

JOURNAL OF THE SOIL MECHANICS AND FOUNDATIONS DIVISION

PROCEEDINGS OF
THE AMERICAN SOCIETY
OF CIVIL ENGINEERS

CONTENTS

→

This Journal is published monthly by the American Society of Civil Engineers. Publications office is at 345 East 47th Street, New York, N.Y. 10017. Address all ASCE correspondence to the Editorial and General Offices at 345 East 47th Street, New York, N.Y. 10017. Allow six weeks for change of address to become effective. Subscription price is $16.00 per year with discounts to members and libraries. Second-class postage paid at New York, N.Y. and at additional mailing offices. SM.

Mechanics and Foundations Division, ASCE, Vol. 98, No. SM3, Proc. Paper 8790, Mar., 1972, pp. 265-290.

APPENDIX II.—NOTATION

The following symbols are used in this paper:

C_u = undrained cohesion, in kilopascals;
E = Young's modulus of ideal elastic soil, in kilopascals;
E_M, E_f, E_0, E_s = pressure meter moduli conventionally defined with Poisson's ratio equal to 0.33 on standard test curve E_M and on "autoforeuse" probe test curve: tangent modulus at failure E_f, initial tangent modulus E_0 and secant modulus at failure E_s, in kilopascals;
F = pressure meter curve function, in kilopascals;
f = stress-strain function, in kilopascals;
I_ρ = index of remolding;
K_0 = coefficient of lateral earth pressure at rest;
P = pressure in probe;
P_0 = initial horizontal pressure;
P_f^* = creep pressure (pression de fluage) in standard test;
P_l = theoretical limit pressure in pressure meter curve;
P_l = conventionnal limit pressure in standard test;
r = initial radial distance in cylindrical coordinates;
u_r = radial displacement;
z = vertical coordinate;
β = shear strength factor for remolded soil;
γ = shear angle;
ϵ = circumferential strain;
ϵ_r = radial strain;
θ = angle coordinate;
λ = function for rest of integral of limit pressure;
ν = Poisson's ratio;
ρ = radial distance in deformed state;
σ_r = radial stress;
σ_z = vertical stress;
σ_θ = circumferential stress; and
τ = maximum shear stress.

Subscripts.

f = failure at contact of probe; and
0 = values at contact of probe.

JOURNAL OF THE SOIL MECHANICS AND FOUNDATIONS DIVISION

Seepage Analysis of Earth Banks Under Drawdown

By Chandrakant S. Desai,[1] M. ASCE

INTRODUCTION

The class of problems known as transient unconfined seepage under drawdown conditions in porous media is analyzed by using a finite element procedure. There are many publications available on general seepage problems; only those publications directly relevant to this category of problems are referenced herein. Although the formulation developed herein is general, it is used for solution of free-surface seepage in long river banks (or dams) subjected to gradual drawdown conditions in the external water levels. This situation has significant applications for stability analyses and computations of fluid flow from banks and dams.

Specifically, the procedure is used for seepage analyses in the pervious banks of the Mississippi River. In designing protective structures for the riverbanks, it is essential to compute precise locations of the changing free surface as a consequence of changes in the river floods. Conventionally, such designs are performed on the basis of sudden drawdown conditions which may result into conservative designs (1,6). The procedure developed herein could allow evaluation of the free surface for gradual (and sudden) drawdown in the riverbanks and thus could provide data for more precise stability analyses.

Two examples are solved by using the proposed finite element procedure. In the first example, the numerical solutions are compared with resultsffrom laboratory experiments with a long parallel-plate viscous-flow model which

Note.—Discussion open until April 1, 1973. To extend the closing date one month, a written request must be filed with the Editor of Technical Publications, ASCE. This paper is part of the copyrighted Journal of the Soil Mechanics and Foundations Division, Proceedings of the American Society of Civil Engineers, Vol. 98, No. SM11, November, 1972. Manuscript was submitted for review for possible publication on December 8, 1971.

[1]Research Civ. Engr., Soil and Rock Mechanics Branch, U.S. Army Engineer Waterways Experiment Station, CE, Vicksburg, Miss.

simulates a long riverbank. The second example involves actual field observations at a section along the banks of the Mississippi River. The U.S. Army Corps of Engineers has installed a number of piezometer stations along the banks and periodic readings of river stages and the corresponding piezometric heads are recorded. The field observations at the section are compared with the solutions from the finite element method.

In dealing with an infinite medium such as a riverbank, the inherent nature of a numerical technique requires that only a significant portion of the infinite medium be included in the analysis as the discretized assemblage (5). The selection of the significant portion requires adequate study and is influenced by various factors. Some criteria for discretization of such infinite media are suggested herein on the basis of the experimental observations and a number of numerical solutions. In order to illustrate the use of the procedure in accounting for different possible soil properties, a series of solutions is obtained for a range of possible permeabilities in a bank section.

Due to many parameters that may require consideration, it is relatively difficult to evolve general design curves from a numerical technique. Design criteria, however, may be developed for situations of common occurrence with common geometric and material properties. Some projections on this topic are also presented.

FINITE ELEMENT FORMULATION

Governing Differential Equation.—The differential equation governing two-dimensional steady flow in a long riverbank or a dam shown schematically in Fig.1 is expressed as (5,10)

$$\frac{\partial}{\partial x}\left(k_x \frac{\partial \psi}{\partial x}\right) + \frac{\partial}{\partial y}\left(k_y \frac{\partial \psi}{\partial y}\right) = 0 \quad \ldots\ldots\ldots\ldots\ldots\ldots\ldots\ldots\ldots\ldots (1)$$

in which k_x and k_y = the coefficients of permeability in the x and y directions,

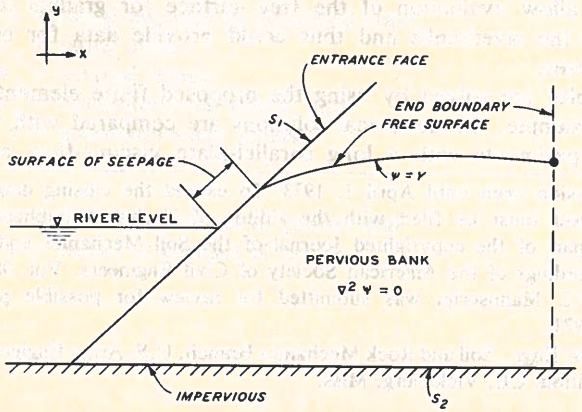

Fig. 1.—Schematic Representation of Flow in Porous Media

respectively; and ψ = the total fluid head. Eq. 1 is based on the Darcy law expressed in matrix form as

$$\{V\} = -[R]\{g\} \quad \ldots\ldots\ldots\ldots\ldots\ldots\ldots\ldots\ldots\ldots\ldots\ldots (2)$$

and on the fulfillment of the continuity conditions in the flow domain (10). In Eq. 2, $\{V\}^T$ = the velocity vector, $[V_x\ V_y]$; $\{g\}^T$ = the vector of gradients, $\left[\frac{\partial \psi}{\partial x}\ \frac{\partial \psi}{\partial y}\right]$; and $[R]$ = the matrix of permeabilities = $\begin{bmatrix} k_x & 0 \\ 0 & k_y \end{bmatrix}$.

The boundary conditions associated with the free-surface flow are (Fig. 1)

$$\psi = \bar{\psi}(t) \text{ on } S_1 \quad \ldots\ldots\ldots\ldots\ldots\ldots\ldots\ldots\ldots\ldots\ldots\ldots (3a)$$

and $$k_x \frac{\partial \psi}{\partial x}\frac{\partial x}{\partial \eta} + k_y \frac{\partial \psi}{\partial y}\frac{\partial y}{\partial \eta} = \bar{Q} \text{ on } S_2 \quad \ldots\ldots\ldots\ldots\ldots\ldots\ldots\ldots (3b)$$

and $\psi = Y(x, y, t)$ on the free surface and on the surface of seepage . . . (3c)

Here S_1 is the part (entrance face) of the boundary on which ψ is prescribed;

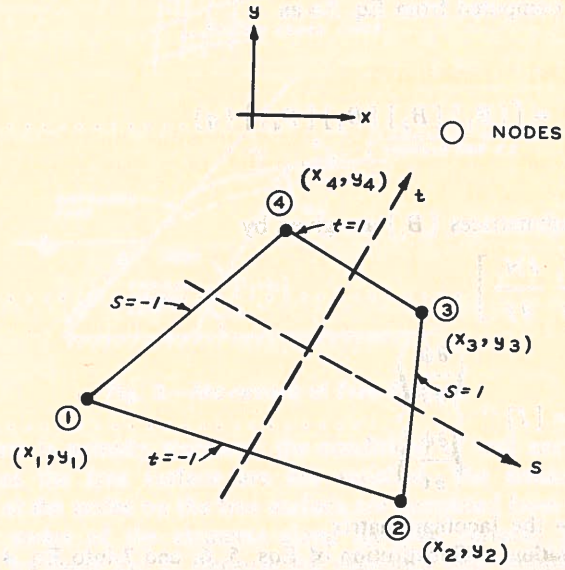

Fig. 2.—Quadrilateral Finite Element

S_2 is the part on which flow, $\bar{Q}$, is prescribed; Y represents the elevation head; and η denotes normal to a boundary.

The variational functional corresponding to the governing Eq. 1 can be expressed as (5,19)

$$A = \iiint_V \frac{1}{2}\left[k_x\left(\frac{\partial \psi}{\partial x}\right)^2 + k_y\left(\frac{\partial \psi}{\partial y}\right)^2\right] dV \quad \ldots\ldots\ldots\ldots\ldots\ldots (4)$$

Finite Element and Field Variable Model.—A four node isoparametric quadrilateral element (Fig. 2) is used (5,7,8). The field variable model describing an approximate variation of ψ within the element is

$$\psi(s,t) = \{N\}^T \{q\} \quad \ldots\ldots (5a)$$

in which s and t are the natural coordinates of the element; $\{N\}^T = [N_1\, N_2\, N_3\, N_4]$ is the vector (or matrix) of interpolation functions; and $\{q\}^T = \{\psi_1 \psi_2 \psi_3 \psi_4]$ is the vector of nodal heads. The values of N_i for the system shown in Fig. 2 are

$$N_i = \frac{1}{4}(1 + ss_i)(1 + tt_i); i = 1, 2, 3, 4 \quad \ldots\ldots (5b)$$

The coordinates x, y of the element are also expressed by using the same interpretation functions

$$\begin{Bmatrix} x \\ y \end{Bmatrix} = \begin{bmatrix} \{N\}^T & 0 \\ 0 & \{N\}^T \end{bmatrix} \begin{Bmatrix} x_n \\ y_n \end{Bmatrix} \quad \ldots\ldots (6)$$

in which $\{x_n\}^T = [x_1\, x_2\, x_3\, x_4]$ and $\{y_n\}^T = [y_1\, y_2\, y_3\, y_4]$. The gradient vector can be computed from Eq. 5*a* as

$$\{g\} = \begin{Bmatrix} \frac{\partial \psi}{\partial x} \\ \frac{\partial \psi}{\partial y} \end{Bmatrix} = [[B_1]\,[B_2]\,[B_3]\,[B_4]]\,\{q\} \quad \ldots\ldots (7a)$$

in which the submatrices $[B_i]$ are given by

$$[B_i]^T = \begin{bmatrix} \frac{\partial N_i}{\partial x} & \frac{\partial N_i}{\partial y} \end{bmatrix} \quad \ldots\ldots (7b)$$

and

$$\begin{Bmatrix} \frac{\partial \psi}{\partial x} \\ \frac{\partial \psi}{\partial y} \end{Bmatrix} = [J]^{-1} \begin{Bmatrix} \frac{\partial \psi}{\partial s} \\ \frac{\partial \psi}{\partial t} \end{Bmatrix} \quad \ldots\ldots (7c)$$

in which $[J]$ = the Jacobian matrix.

Element Equations.—Substitution of Eqs. 5, 6, and 7 into Eq. 4 yields

$$A = \{q\}^T \iiint_V [B^T]\,[R]\,[B] \det([J])\,\{q\}\, dsdt \quad \ldots\ldots (8)$$

Extremization of A in Eq. 8 gives the element equations for steady-state seepage

$$[k]\,\{q\} = 0 \quad \ldots\ldots (9)$$

in which $[k] = \iiint_V [B^T]\,[R]\,[B] \det([J])\, dsdt$ and is referred to as element permeability matrix (5), and $\{q\}$ = vector of element nodal heads.

The assemblage equations are obtained by adding element equations by using the direct stiffness method. Such assemblage equations after introduction of the boundary conditions such as $\psi = \bar{\psi}(t)$ (Eq. 3*a*) can be written as

$$[K]\,\{r\} = \{R\} \quad \ldots\ldots (10)$$

in which $[K]$ = assemblage permeability matrix, $\{r\}$ = assemblage nodal head vector; and $\{R\}$ = assemblage nodal forcing parameter vector. Natural boundary conditions such as Eq. 3*b* are automatically satisfied in the variational formulation.

Determination of Changing Free Surface.—Under a small change in the external head, (Fig. 3) the free-surface experiences corresponding movements. In the solution scheme, the transient problem is divided into a number of steady-state problems and Eq. 10 is solved to obtain values of nodal heads and velocities for a given time level. The domain of flow for such solution is defined by the free surface at that time and the impervious boundaries (Fig. 1).

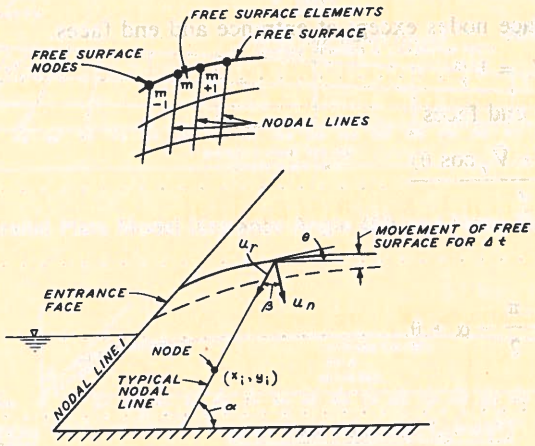

Fig. 3.—Movement of Free Surface

As the problem is actually transient, the conditions of null normal flow and velocity across the free surface are not satisfied. The nonzero values of the velocities at the nodes on the free surface are computed from the computed heads at the nodes of the elements along the free surface. The velocities are evaluated by using Eq. 2. Because the velocities thus computed are those based on Darcy's law, the actual particle velocities need be computed (2,3,5,9,11). The particle velocity vector $\{V_p\}$ is obtained as

$$\{V_p\} = \frac{1}{f}\{V\} \quad \ldots\ldots (11)$$

in which f = porosity of the medium.

The normal movements of the particles at the free-surface nodes are computed by multiplying the normal component of the velocity, Eq. 12 following, by a given time increment Δt. This permits evaluation of the new coordinates

of the free-surface nodes. A new finite element mesh is now generated by modifying the coordinates of the nodes in the flow domain. To facilitate such modifications, a number of nodal lines (Fig. 3) are fixed by assigning angles α which they subtend with a bottom boundary. These lines retain their orientation during the drawdown. Further simplification is obtained by locating the nodes along a nodal line at equal vertical and horizontal distances. The procedure can permit modification of coordinates of a portion of the mesh in the neighborhood of the free surface. The mesh in the zones that may not experience movements can be kept fixed. The following equations summarize the process of modification of the mesh:

$$\left.\begin{array}{l}\bar{V}_x = \dfrac{V_x^m + V_x^{m+1}}{2}\\[2ex] \bar{V}_y = \dfrac{V_y^m + V_y^{m+1}}{2}\end{array}\right\} \quad \ldots\ldots\ldots \quad (12a)$$

for all free-surface nodes except at entrance and end faces.

$$\bar{V}_x = V_x^m \text{ and } \bar{V}_y = V_y^m \quad \ldots\ldots\ldots \quad (12b)$$

at entrance and end faces

$$V_n = \frac{(\bar{V}_x \sin\theta + \bar{V}_y \cos\theta)}{f} \quad \ldots\ldots\ldots \quad (12c)$$

$$u_n = V_n \cdot \Delta t \quad \ldots\ldots\ldots \quad (12d)$$

$$u_r = \frac{u_n}{\cos\beta}, \beta = \frac{\pi}{2} - \alpha + \theta \quad \ldots\ldots\ldots \quad (12e)$$

$$u_x = u_r \cos\alpha \quad \ldots\ldots\ldots \quad (12f)$$

$$u_y = u_r \sin\alpha \quad \ldots\ldots\ldots \quad (12g)$$

$$x_i^j = x_i^{j-1} + u_x \quad \ldots\ldots\ldots \quad (12h)$$

$$y_i^j = y_i^{j-1} + u_y \quad \ldots\ldots\ldots \quad (12i)$$

in which i denotes a nodal point, and j denotes a time level. Other symbols are explained in Fig. 3. As the field variable model, Eq. 5, yields discontinuous velocities at a node between two elements, an average of the velocities at that node is adopted for computing the foregoing movements (first two equations of Eq. 12). A number of iterations may be performed at each time increment in order to improve satisfaction of the conditions at the free surface, Eq. 3c (5,18). If the time interval is small, one to three iterations are sufficient for an acceptable solution.

Similar procedures have been recently employed by France, et al. (9) for steady unconfined and sudden drawdown analyses. Neuman and Witherspoon (17) have used a finite element iterative procedure for unsteady seepage with

a free surface. It is based on an averaging scheme that leads to a stable higher order time integration.

APPLICATIONS

Example 1, Comparisons with Laboratory Tests.—A number of experiments were performed with a large parallel plate viscous flow model. The model simulated a long pervious riverbank. Models with various entrance slope angles were tested. A typical result for slope angle equal to 45° is included herein. The approximate length and height of this model were 300 cm and 50 cm, respectively (Fig. 4). The level of fluid in the reservoir in the model was raised at a certain rate, allowed to stabilize at 25 cm height of fluid, and

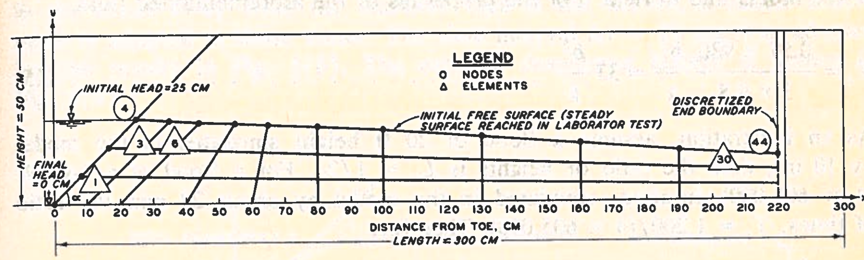

Fig. 4.—Parallel Plate Model (Entrance Angle 45°) and Finite Element Mesh

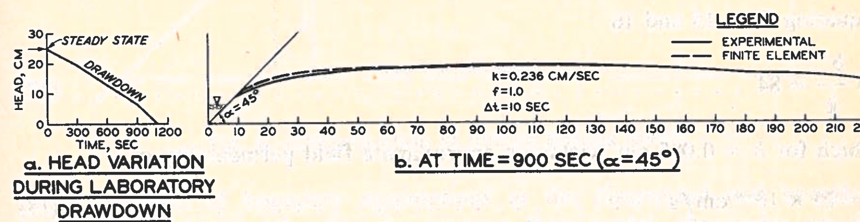

Fig. 5.—Comparison of Results and Variation of External Head

then was allowed to fall as shown in Fig. 5(a). The movements of the free surface were recorded photographically. The fluid used was silicone fluid, which is found to experience little fluctuations in its properties with ambient temperature changes (3,4).

The equation governing the flow through the model is analogous to Eq. 1, in which the equivalent permeability of the model, k_m, is obtained as (6,10)

$$k_m = \frac{b^2 \rho g}{3\mu} \quad \ldots\ldots\ldots \quad (13)$$

in which b = half width of gap; ρ = the density of the fluid, 0.97 gm/cm^3; g = the gravitation constant, 980 cm/s squared; and μ = 9.8 poises is

the viscosity. The average value of b was found equal to 0.085 cm, which yields k_m = 0.236 cm/s, and a value of unity was adopted for the porosity f of the model.

Equivalent Field Permeability.—Details of derivation of the procedure for computing the field permeability equivalent to a given model dimensions and fluid properties are described in Refs. 3 and 4. Only brief computations for equivalent field permeability are described. The ratio of model velocity V_m and field velocity, V, is

$$V_r = \frac{V_m}{V} = \frac{b^2 \rho_m g}{3 k \mu_m} \quad (14)$$

The fluid in the field is assumed to be water and same gradients are assumed in the model and in field. For the properties of the aforementioned fluid

$$V_r = \frac{0.97 \times 980}{3 \times 9.8} \frac{b^2}{k} \simeq 33 \frac{b^2}{k} \quad (15)$$

As an illustration, assume a flood of 20 ft height simulated in the model by 10 in., then the ratio of heights is L_r = 1/24. For a flood of a 4-week (4 × 605,000) duration, simulated in the model by about 20 min the ratio of times, T_r = 1,200/(4 × 605,000). Therefore

$$V_r = \frac{L_r}{T_r} = 84 \quad (16)$$

Equating Eqs. 15 and 16

$$33 \frac{b^2}{k} = 84 \quad (17)$$

which for b = 0.085 cm, yields an approximate field permeability of

$$k \simeq 25 \times 10^{-4} \text{ cm/s} \quad (18)$$

which is representative of permeability of fine sands in the Mississippi riverbanks under consideration.

Finite Representation of Infinite Media.—An important question arises as to what extent of the flow region should be discretized for the finite element solution. During the laboratory tests, it was observed that the changes in the reservoir head did not affect significantly the movements of the points in regions at a distance of about 10 times the total magnitude of change in the external level. In other words, for the model test (Fig. 4) the total change in external head was 25 cm. Around distances of about 200 cm measured from the final point reached after drawdown (in this case the toe of the model), the free surface did not experience significant movements during the drawdown. In order to further examine this observation, numerical results from the finite element analysis for three different distances, 190 cm, 220 cm, and 250 cm were obtained. On the basis of the experimental and numerical results, it seems that acceptable solutions can be obtained by placing the

end boundary at a distance of about $8H$-$12H$ from the final drawdown (Fig. 6) in which H = total drawdown.

An impervious bottom boundary is physically available for the viscous flow model. However, for deep porous media in the field, it is necessary to select adequate location for the bottom boundary (Fig. 6) which is assumed to be impervious in the formulation. On the basis of the numerical solution, it was observed that at a depth of about $4H$ from the final drawdown point, the computed heads along vertical sections showed little change. Thus, if the bottom boundary is located in the range of about $3H$-$6H$, it can provide an approximate impervious boundary (Fig. 6).

Finite Element Analysis.—The end boundary was placed at 220 cm from the toe. The finite element mesh is shown in Fig. 4. It contains 30 elements and 44 nodes. As in a problem of this nature, the variation of gradients in the zones away from the entrance face is not severe, a rather coarse mesh is adopted in those zones. The time interval Δt = 10 sec was adopted for the results in Fig. 5(b). The external drawdown history is shown in Fig. 5(a).

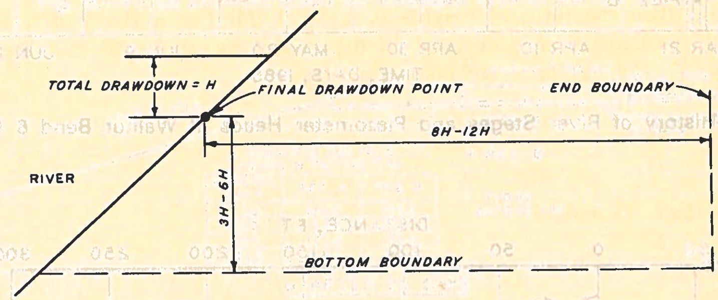

Fig. 6.—Discretization of Infinite Porous Media

The question of boundary assumptions at the discretized end boundary is analyzed subsequently. For the viscous flow model, the nodes on the end boundary were fixed, but the heads at those nodes were permitted to vary. Fixing of the nodes on the end boundary was guided by the fact that the free-surface points around that distance did not move significantly during the drawdown. Fig. 5(b) shows a comparison between the finite element solution and the experimental results for a typical time level of 900 sec during drawdown. The correlation between the two results is considered to be good.

Example 2, Comparisons with Field Observations.—The U.S. Army Corps of Engineers has installed piezometers along a number of sections on the Mississippi River. The histories of river stages and the corresponding heads of water in the piezometers are recorded over periods of time. A typical history at a section called Walnut Bend 6 for a part of the year 1965 is shown in Fig. 7 (1). This figure indicates the variation in river level and the corresponding heads in two piezometers A and B installed in a well at a distance of about 30 ft from the top of the bank. Fig. 8 shows the location

of the piezometers, the cross section of the river at Walnut Bend 6, and the log of borings at the section. The bank at this section consists of predominantly silty fine sand (ML). The U.S. Army Corps of Engineers has performed investigations (12,13,15) for evaluation of the permeabilities and porosities of the soils in the regions in the vicinity of the Mississippi River. The coefficient of permeability and the porosity of the soil at Walnut Bend 6 section were estimated to be of the order of 10×10^{-4} cm/s to 20×10^{-4} cm/s (2.84 ft/day to 5.68 ft/day) and 0.4, respectively.

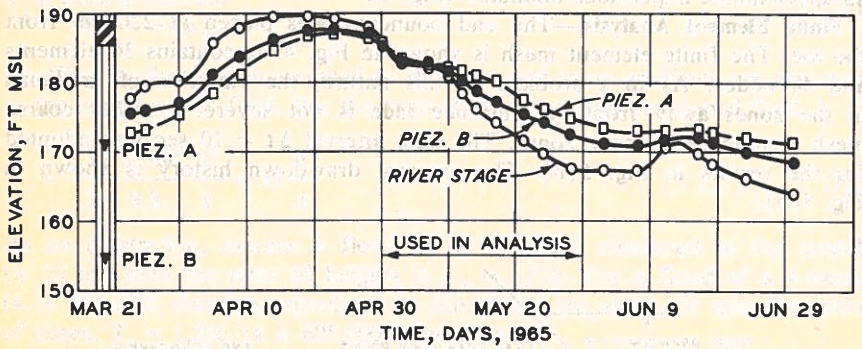

Fig. 7.—History of River Stages and Piezometer Heads at Walnut Bend 6 (From Ref. 1)

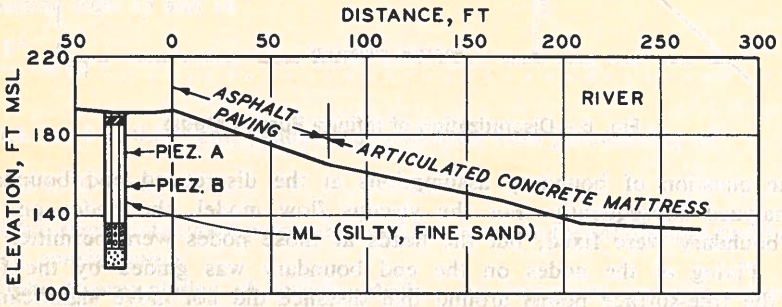

Fig. 8.—Cross Section at Walnut Bend 6 and Boring Log (From Ref. 1)

The drawdown in the river level from April 30 to May 30, 1965 (Fig. 7) was considered for the analysis herein. In this time period of 30 days the river level fell from about El. 187.5 to El. 167.5, at an average rate of about 0.67 ft/day. Assuming that the section was porous to a large distance across the river and assuming that the flood stayed long enough for the free surface to develop, the steady-free surface was estimated as shown in Fig. 9. Such steady-free surface can be estimated either on the basis of experimental observations (4) or from a conventional analysis (10) or by using the finite element method (2,18), or by using other numerical techniques (6).

The section in Fig. 8 was idealized as shown in Fig. 9 and the mesh contained 48 elements and 63 node points. On the basis of the observation of the model tests stated above, the infinite bank was represented by a finite region (Fig. 9) which was terminated at 400 ft from the toe of the bank. This distance was about 13 times the maximum fall $H = 20$ ft in the river level, as measured from the final point of drawdown. The bottom boundary was placed at a distance of about $4H$ measured from the final

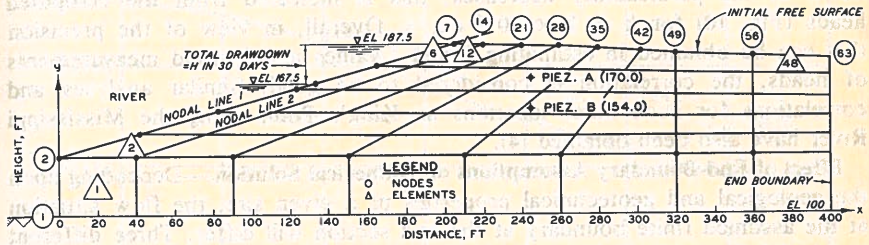

Fig. 9.—Finite Element Mesh for Idealized Walnut Bend 6 Section

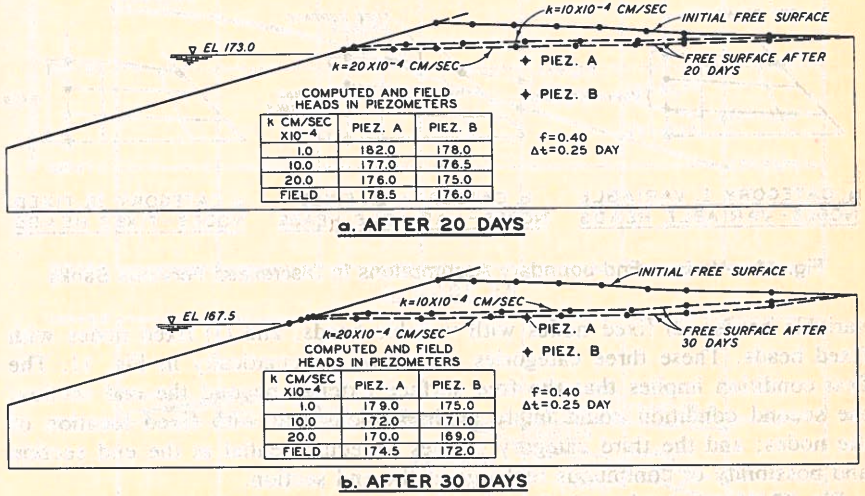

k CM/SEC X10⁻⁴	PIEZ. A	PIEZ. B
1.0	182.0	178.0
10.0	177.0	176.5
20.0	176.0	175.0
FIELD	178.5	176.0

k CM/SEC X10⁻⁴	PIEZ. A	PIEZ. B
1.0	179.0	175.0
10.0	172.0	171.0
20.0	170.0	169.0
FIELD	174.5	172.0

Fig. 10.—Comparisons of Computed and Field Heads in Piezometers at Walnut Bend 6

drawdown point. At the end boundary, the nodes were fixed but the nodal heads were permitted to vary. A time interval $\Delta t = 0.25$ days was adopted.

Comparisons.—Fig. 10 shows location of the free surface at typical time levels of 20 and 30 days during drawdown for $k = 10 \times 10^{-4}$ and 20×10^{-4} cm/s. The piezometers A and B are located at approximate elevations of 174.0 and 154.0, respectively. Their locations are marked in Fig. 9. In Fig. 10 are shown the computed values of heads in the piezometers in comparison

with the field observations. The computed values were averaged from the heads at the nodes in the vicinity of a piezometer at a certain time level. The computed values of heads for the foregoing range of permeability at the Walnut Bend section show good correlation with the field observations. The correlation between the numerical and field results is better in the initial times during drawdown than in the final times. Also, for the field permeabilities of 10 to 20 $\times$ 10^{-4} cm/s, the movement of the free surface seems to be faster compared with the observed piezometer heads. The movement slows down as the permeability decreases; this is indicated from the computed heads (Fig. 10) for $k = 1 \times 10^{-4}$ cm/s. Overall, in view of the precision that can be obtained in estimating k and f values and in field measurements of heads, the correlation is considered to be good. Similar analyses and correlations for such other locations as King's Point along the Mississippi River have also been obtained (4).

Effect of End-Boundary Assumptions on Numerical Solution.—Depending upon the geological and geotechnical properties of a given site, the flow situation at the assumed finite boundary at the end section will differ. Three different types of boundary assumptions are delineated herein: (1) Variable nodes with

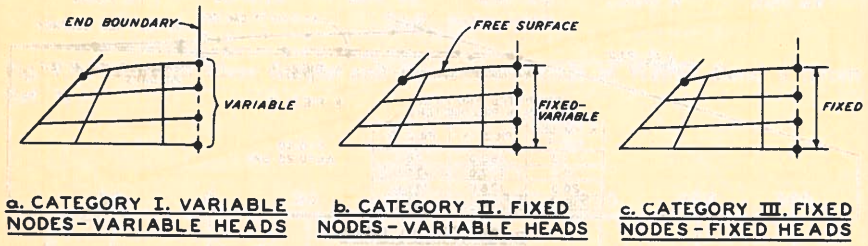

Fig. 11.—Various End-boundary Assumptions in Discretized Pervious Banks

variable heads; (2) fixed nodes with variable heads; and (3) fixed nodes with fixed heads. These three categories are shown schematically in Fig. 11. The first condition implies that the free surface extends beyond the end section; the second condition could imply an impervious end with fixed location of the nodes; and the third category implies an equipotential at the end section and possibility of continuous recharge at the end section.

Fig. 12 compares the solutions for the mesh shown in Fig. 9 for the three different categories. The results shown are for a typical time level of 20 days, $k = 5.64$ ft/day and $f = 0.4$. The figure shows the movement of typical nodes 14, 28, and 56 for the three categories. The vertical coordinates or height of the nodes for various time levels are plotted; whereas, the horizontal coordinates are shown in the parentheses.

The results for the first two categories show no significant difference. The results for the third category are significantly different from the other two. Both the first and second category seem to be suitable for long pervious banks. In the foregoing analyses, the second category is adopted. This assumption also permits some reduction in computations. The assumption

in the third category would be suitable for analysis of drawdown on a face of a dam when the water level at the other face remains constant and provides an equipotential.

Analysis for Different Permeabilities.—The banks of the Mississippi River in the zones of interest usually contain fine sands. The coefficients of

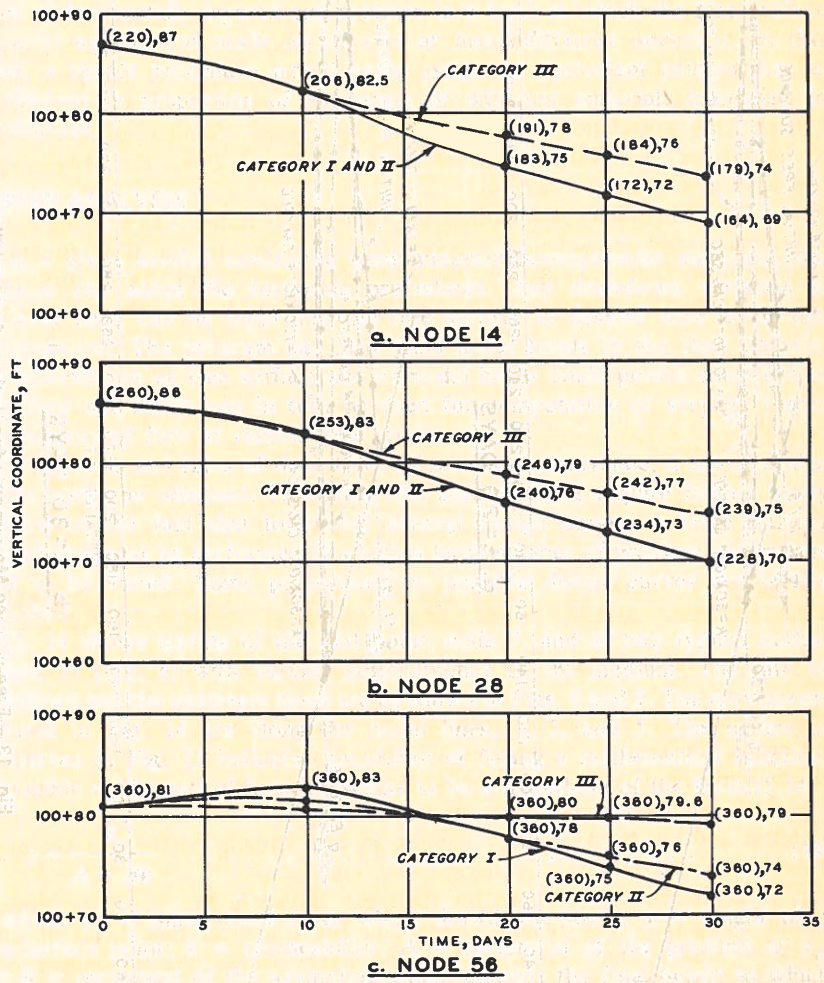

Fig. 12.—Comparisons of Movements of Typical Free-surface Nodes for Various Categories (Fig. 11)

permeability for these sands are assumed to fall in the range of 1×10^{-4} cm/s (0.284 ft/day) to 100×10^{-4} cm/s (28.4 ft/day). Fig. 13 shows locations of free surface for mesh in Fig. 9 at typical time levels of 20 and 30 days for different coefficients of permeability, 0.284 ft/day, 2.84 ft/day, 5.68 ft/day,

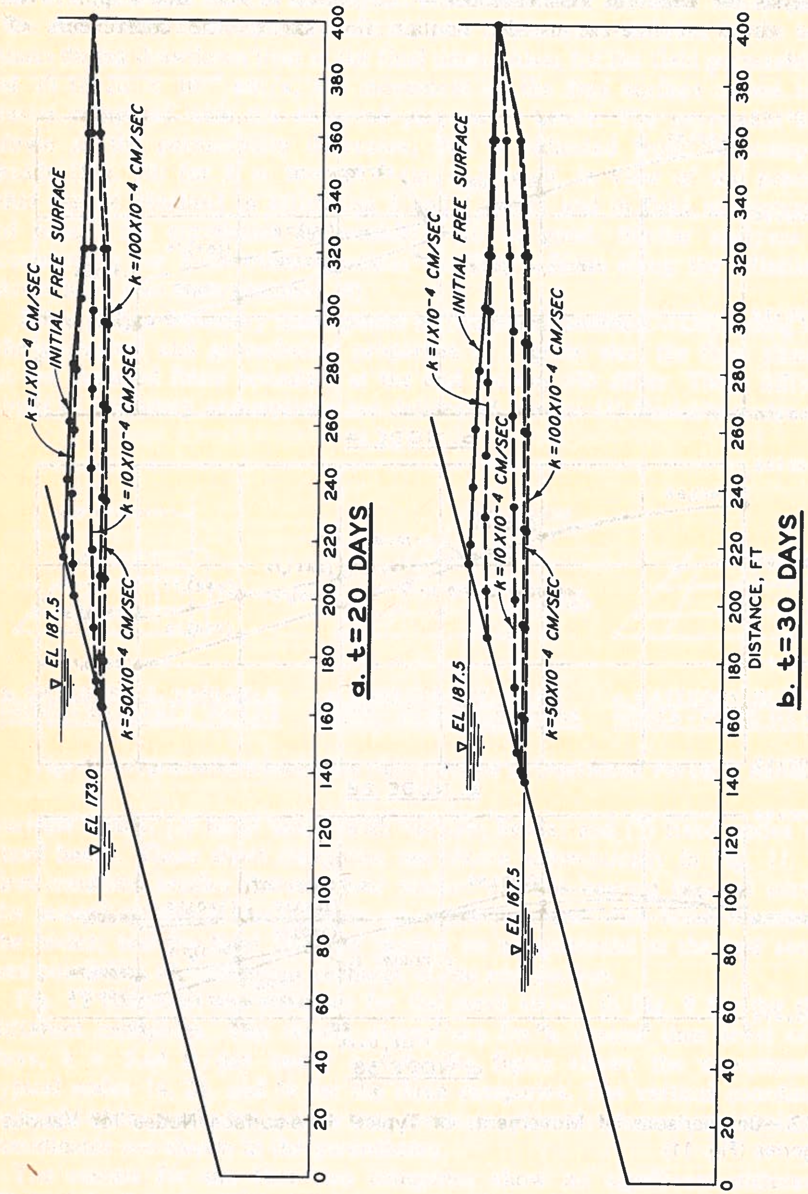

Fig. 13.—Free-surface Movements for Various Permeabilities

16.4 ft/day, and 28.4 ft/day. The results for k = 2.88 ft/day lie between those for k = 1.44 ft/day and 7.2 ft/day. The porosity was assumed to be equal to 0.4. It can be seen that the free surfaces moves faster with increasing permeability.

Nonhomogenities in Bank.—In the cases where the free surface does not cross an interface between different soils in a bank, the proposed procedure could be directly applied. Certain modifications would be required in the event of horizontally layered soil systems in a bank in which the free surface traverses an element made up of two or more different materials. In this event, a simple procedure would be to assign an equivalent permeability to an element in proportion of the areas of different materials contained in the element.

DESIGN ANALYSIS

For a given section containing predominantly homogeneous materials, the designer can adopt the foregoing procedures. Any drawdown variation in the river head can be input and the free surface at desired time levels can be computed. The program can also yield nodal heads in the flow domain. The information on free surface and on nodal heads could permit construction of a flow net which can in turn be used for computation of seepage forces and quantity of flow at various time levels.

For sections and rates of drawdown of common occurrence, a set of design curves could be obtained. However, this aspect would require further study in view of the fact that to evolve general design curves, a large number of analyses must be performed in which a large number of problem parameters need to be varied. Some projections on possible design curves are briefly described.

Fig. 14 shows travels of the exit point, node 7, and of two typical nodes, 28 and 35 (Fig. 8) with various permeabilities of the medium. The rate of drawdown and the upstream slope are as shown in Figs. 8 and 9. The movements depicted in Fig. 14 are along the nodal lines, 1, 3, and 5. The nature of the curves in Fig. 13 indicates possibility of fitting a mathematical function. A possible mathematical function seems to be a hyperbola of the form (5,14)

$$y_o - y = \frac{k}{A + Bk} \qquad (19)$$

in which y_o = initial head from where drawdown starts; y = height of a free-surface point; k = permeability; A = reciprocal of the gradient at y_o; and B = reciprocal of the asymptote which denotes the final height to which the point may have reached. The time dependence may be incorporated as

$$y_o - y = \frac{kCt^n}{1 + BCkt^n} \qquad (20)$$

in which $1/A = Ct^n$; C = parameter determined from a plot of g_o, the initial gradient; and t = time in days. Determination of the parameter $A, B, C,$ and n for a number of points for a given section and ratio of drawdown

can permit evaluation of travel of the points during drawdown from Eq. 20. The free surfaces can be sketched on the basis of the positions of a number of such typical points. This suggestion however, will require further investigations and validation.

Computer Programs.—Although the formulation has been employed only for transient unconfined seepage under gradual drawdown conditions, it is general and can be conveniently used for other categories of seepage such as steady confined and steady unconfined seepage. A set of computer codes

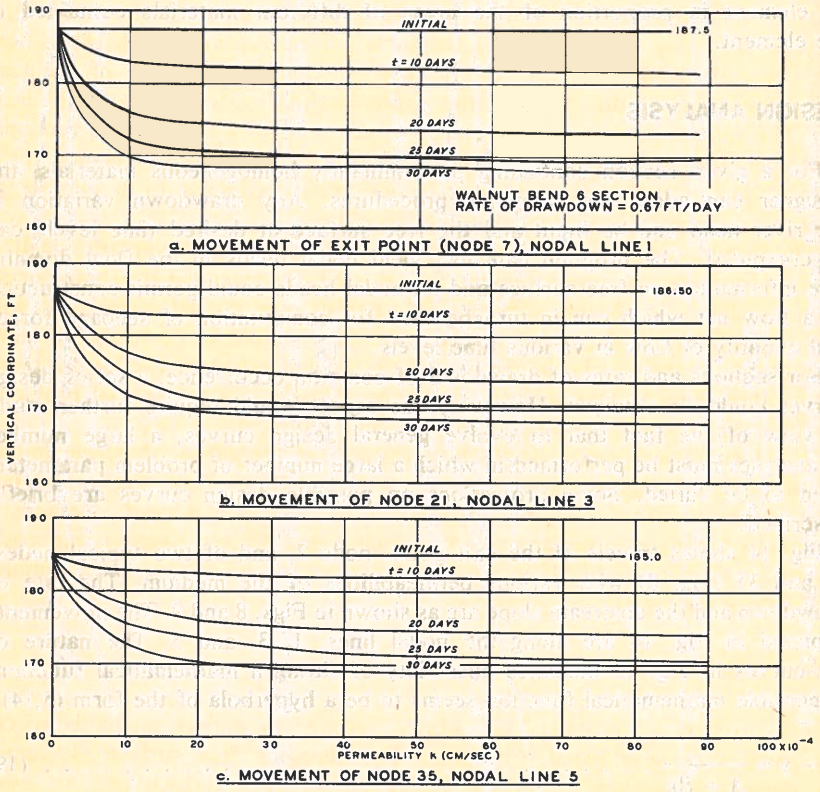

Fig. 14.—Movements of Typical Free-surface Nodes

have been developed at WES to handle these categories (2). It is found that these codes are efficient and compact. For instance, on the GE 430 computer which is a relatively slow machine, the entire problem of tracing the history of free surfaces for the Walnut Bend section took about 15 min of time at a cost of about $30. This time includes both compile and execution times. On a faster computer, the computational time could be reduced. The code do not use tapes and the banded equation set is solved by using symmetric Gauss-Doolittle procedure (5).

COMMENTS

The time integration scheme used here is essentially similar to the forward difference procedure, and is subjct to numerical instability beyond a certain range of discretization. A number of factors such as spatial and timewise subdivision, permeability and rate of drawdown or rise of external fluid head can influence the stability behavior. Within the range of spatial and temporal discretization an user may adopt irrespective of the integration scheme, the proposed procedure provides solutions of acceptable accuracy. For instance, in the foregoing practical problem, an user may not usually adopt a mesh coarser than that shown in Fig. 9, and a time interval smaller than 0.25 day or 0.50 day. It seems that within a practical range of discretization, the class of problems is not significantly affected by the order of the time integration nor by the order of the approximating model for the fluid head (4). The general question of the choice of the scheme with optimum economy and accuracy from among a number of available numerical schemes for a given class of problems is wide in scope and is affected by a number of factors which will require detailed investigations.

The formulation presented herein is applicable also to axisymmetric idealizations. Moreover, the procedure can be conveniently extended for three-dimensional analysis (9). A three-dimensional analysis may not be economical with the capabilities of the present generation of computers. Fortunately, many practical problems can be solved by using plane and axisymmetric idealizations, and a three-dimensional analysis may become necessary for special problems such as seepage through junction of dam and abutment.

The formulation yields satisfactory results for the range of permeabilities considered. For highly porous materials with non-Darcy flow, the formulation may need modifications, McCorquodale (16). The isoparametric element is found to facilitate formulation and computational efforts. Only in the cases when an element is highly narrow and not well conditioned, computational difficulties may arise.

CONCLUSIONS

The problem of unsteady unconfined seepage in porous media is solved by using a finite element procedure. The changing free surface is located by computing movements of the nodes on the free surface and by using an iterative scheme. The numerical solutions are in good agreement with laboratory tests and with field observations. Various boundary assumptions possible in long porous banks are examined. Consideration is given to the significant question of discretization of infinite media. Attention is directed toward developing an economical computer procedure for design analysis. On the basis of a number of numerical solutions, it is believed that a reasonable mesh with a lower order approximating function such as the one used herein (Eq. 5), would provide a solution with acceptable accuracy and economy. For engineering solution, it may not be necessary to use higher order approximating functions which involve greater computational and formulation efforts. Finally, the satisfactory correlation between the numerical solutions

and field observations would enhance the usefulness of the finite element method for practical stability analysis of banks and dams.

ACKNOWLEDGMENTS

The results described herein were obtained from research conducted under the project on seepage studies in the Mississippi Riverbanks supported by the U.S. Army Engineer Division, Lower Mississippi Valley (LMVD) of the U.S. Army Corps of Engineers by the Waterways Experiment Station (WES), Vicksburg, Miss. The permission granted by the chief of Engineers to publish this information is appreciated. Useful comments and suggestions by W. C. Sherman and W. E. Strohm of WES, R. I. Kaufman and F. J. Weaver of LMVD, and R. S. Sandhu of Ohio State University are gratefully acknowledged.

APPENDIX I.—REFERENCES

1. Clough, G. W., "Ground Water Level in Silty and Sandy Mississippi Upper Banks," *Report*, Mississippi River Commission, Corps of Engineers, Vicksburg, Miss., Aug., 1966.
2. Desai, C. S., "Finite Element Procedures for Seepage Analysis Using an Isoparametric Element," *Proceedings of the Symposium on Applications of the Finite Element Method to Problems in Geotechnical Engineering*, U.S. Army Engineer Waterways Experiment Station, Vicksburg, Miss., May, 1972.
3. Desai, C. S., "Seepage in Mississippi Riverbanks, Report 1, Analysis of Transient Seepage Using Viscous Flow Model and Numerical Methods," *Miscellaneous Paper S-70 3*, U.S. Army Engineer Waterways Experiment Station, CE, Vicksburg, Miss., Feb., 1970.
4. Desai, C. S., "Seepage in Mississippi Riverbanks, Report 2, Analysis of Transient Seepage Using Viscous Flow Model and Numerical Methods," under publication, U.S. Army Engineer Waterways Experiment Station, CE, Vicksburg, Miss.
5. Desai, C. S., and Abel, J. F., *Introduction to the Finite Element Method*, Van Nostrand Reinhold Co., New York, N.Y., 1972.
6. Desai, C. S., and Sherman, W. C., Jr., "Unconfined Transient Seepage in Sloping Banks," *Journal of the Soil Mechanics and Foundation Division*, ASCE, Vol. 97, No. SM2, Proc. Paper 7915, Feb., 1971, pp. 357-373.
7. Ergatoudis, I., Irons, B. M., and Zienkiewicz, O. C., "Curved, Isoparametric, 'Quadrilateral' Elements for Finite Element Analysis," *International Journal of Solids Structures*, Vol. 4, 1968, pp. 32-42.
8. Farhoomand, I., and Wilson, E., "A Nonlinear Finite Element Code for Analyzing the Blast Response of Underground Structures," *Contract Report N-70-1*, U.S. Army Engineer Waterways Experiment Station, CE, Vicksburg, Miss., Jan., 1970.
9. France, P. W., Parekh, C. J., Peters, J. C., and Taylor, C., "Numerical Analysis of Free Surface Seepage Problems," *Journal of the Irrigation and Drainage Division*, ASCE, Vol. 97, No. IR1, Proc. Paper 7959, Mar., 1971, pp. 165-179.
10. Harr, M. E., *Groundwater and Seepage*, McGraw-Hill Book Co., New York, N.Y., 1962.
11. Herbert, R., and Ruston, K. R., "Ground Water Flow Studies by Resistance Networks," *Geotechnique*, Vol. 16, No. 1, Mar., 1966, pp. 53-75.
12. Hvorslev, M. J., "Time Lag and Soil Permeability in Ground Water Observations," *Bulletin No. 36*, U.S. Army Engineer Waterways Experiment Station, CE, Vicksburg, Miss., Apr., 1951.
13. "Investigations of Underseepage and Its Control, Lower Mississippi River Levees," *Technical Memorandum No. 3-424*, Vol. 1 and 2, U.S. Army Engineer Waterways Experiment Station, CE, Vicksburg, Miss., Oct., 1956.

14. Kondner, R. L., "Hyperbolic Stress Strain Response: Cohesive Soils," *Journal of the Soil Mechanics and Foundations Division*, ASCE, Vol. 89, No. SM1, Proc. Paper 3429, Feb., 1963, pp. 115-143.
15. Krinitzsky, E. L., and Wire, J. C., "Groundwater in Alluvium of the Lower Mississippi Valley (Upper and Central Areas)," *Technical Report No. 3-658*, Vol. 1, U.S. Army Engineer Waterways Experiment Station, Vicksburg, Miss., Sept., 1964.
16. McCorquodale, J. A., "Variational Approach to Non-Darcy Flow," *Journalof the Hydraulics Division*, ASCE, Vol. 96, No. HY11, Proc. Paper 7694, Nov., 1970, pp. 2265-2278.
17. Neuman, S. P., and Witherspoon, P. A., "Analysis of Nonsteady Flow with a Free Surface Using the Finite Element Method," *Journal of Water Resources Research*, Vol. 7, No. 3, June, 1971, pp. 611-623.
18. Taylor, R. L., and Brown, C. B., "Darcy Flow Solutions with a Free Surface," *Journal of the Hydraulics Division*, ASCE, Vol. 93, No. HY2, Proc. Paper 5126, Mar., 1967, pp. 25-33.
19. Zienkiewicz, O. C., and Parekh, C. J., "Transient Field Problems: Two-Dimensional and Three Dimensional Analysis by Isoparametric Finite Elements," *International Journal of Numerical Methods in Engineering*, Vol. 2, No. 1, Jan., 1970.

APPENDIX II.—NOTATION

The following symbols are used in this paper:

A = functional;
$[B]$ = matrix;
b = half width of gap in viscous flow model;
f = porosity;
g = gravitational constant, gradient of fluid head;
$\{g\}$ = vector of gradients;
$[J]$ = Jacobian matrix;
$[K]$ = assemblage permeability matrix;
k = coefficient of permeability, L/T;
$[k]$ = element permeability matrix;
L_r = ratio of lengths;
$[N]$ = matrix of interpolation functions;
Q = fluid flux;
$\{q\}$ = vector of nodal heads;
$\{R\}$ = assemblage forcing parameter vector;
$[R]$ = matrix of permeabilities;
$\{r\}$ = assemblage nodal head vector;
S = boundary;
s = natural coordinate;
T_r = ratio of times;
t = time coordinate, natural coordinate;
u = displacement of free surface;
V = Darcian velocity, volume;
V_p = particle velocity;
V_r = velocity ratio;
$\{V\}$ = vector of components of velocity;
x = space coordinate;
Y = elevation of free surface;

y = space coordinate;
α = angle of nodal line;
β = angle between normal to free surface and nodal line;
θ = slope at a point on free surface;
μ = viscosity of fluid;
ρ = fluid density; and
ψ = fluid head.

JOURNAL OF THE SOIL MECHANICS AND FOUNDATIONS DIVISION

Strength Properties of Chemically Solidified Soils

By James Warner,[1] M. ASCE

INTRODUCTION

Although chemical grouting is not new, the great preponderance of applications have been for the primary purpose of subsurface water cut off. Similarly, the majority of past research and literature have been directed toward such practice. Another important use for chemical grouting, although not as well documented, is the in-place strengthening of a soil mass. In spite of the fact that considerable work has been done for this purpose, relatively little data have been developed concerning the strength properties or behavior of chemically solidified soils. In fact, strength increase of soil has often been considered an additional benefit of grouting, being secondary to water cut-off. Accordingly, many manufacturers of chemical grout and grouting specialists themselves have emphasized the use of their products for water control work and relatively little has been done to formulate or evaluate chemical grout materials specifically for use in strength increase applications. Although several authors have attempted to compare the strength properties of solidified soils utilizing various chemical grout materials and systems; the resulting data have often been misleading, due to a total lack of uniformity of test specimen preparation, curing time and environment, and method of testing.

Though many chemical grout systems are used for strength increase, as well as water control, the requirements differ very fundamentally for each purpose. The formation of soft flexible gels and the ability to be used with very short gel times are frequently advantageous in water control work.

Note.—Discussion open until April 1, 1973. To extend the closing date one month, a written request must be filed with the Editor of Technical Publications, ASCE. This paper is part of the copyrighted Journal of the Soil Mechanics and Foundations Division, Proceedings of the American Society of Civil Engineers, Vol. 98, No. SM11, November, 1972. Manuscript was submitted for review for possible publication on September 30, 1971.

[1]Pres., Warner Engineering Services, Intrusion Pressure Grouting Specialists, Los Angeles, Calif.